

# Communication

## A Reaction Model for Prediction of Inclusion Evolution During Reoxidation of Ca-Treated Al-Killed Steels in Tundish

YING REN, LIFENG ZHANG, HAITAO LING,  
YI WANG, DONGTENG PAN, QIANG REN,  
and XINCHENG WANG

A reaction model was developed to investigate evolutions of steel chemistry and inclusion compositions during reoxidation of Ca-treated Al-killed steels in a tundish. The evolutions of  $\text{Al}_2\text{O}_3$ , CaO, MgO, and CaO in inclusions were accurately predicted using the current reaction model. The reaction model can widely predict the evolution of inclusions during tundish reoxidation of Ca-treated Al-killed steels with varying concentrations of Al, Ca, and absorbed oxygen.

DOI: 10.1007/s11663-017-0970-4

© The Minerals, Metals & Materials Society and ASM International 2017

Performance of steel products is significantly affected by the steel cleanliness.<sup>[1–3]</sup> As an essential refining vessel, the continuous casting tundish shows good metallurgical functions for regulating the flow pattern of the molten steel and the removal of inclusions.<sup>[4,5]</sup> Tundish is also known to cause the contamination of the molten steel by a complicated combination of various factors, including entrainment of ladle slag, reaction with tundish cover powders, erosion of refractories, reaction with ladle well packing materials, and air absorption.<sup>[6]</sup> During casting transitions such as cast start and ladle change process, the air absorption can hardly be avoided.<sup>[7]</sup> Reoxidation of the molten steel in the tundish might lead to the increase of oxygen in the steel, the generation of inclusions, and change of inclusion chemistry, which is detrimental in producing high-quality steel grades.<sup>[8–13]</sup> Accurate ability to predict compositions of steel and inclusions in the

tundish is of great importance to better understand the evolution mechanism of inclusions and improve the steel cleanliness.

A large number of physical modeling and mathematical simulation works have been carried out to investigate the flow, temperature field, and removal of inclusions.<sup>[14–18]</sup> It was regretful that chemical composition of inclusions was not accounted for in above investigations due to complicated calculations and lack of thermodynamic data in the multicomponent system. Recently, with the application of thermodynamic software, the formation of inclusions at different temperatures and varying steel compositions in a multicomponent system can be apace and accurately predicted.<sup>[19–22]</sup> There have been several kinetic models developed using the combination of thermodynamic calculations with simplified fluid dynamic equations of the liquid melt, which can be used to predict the evolution of steel chemistry and inclusion compositions during refining process such as ladle furnace<sup>[23–29]</sup> and Ruhrstahl-Heraeus.<sup>[30]</sup> However, there was no available reaction model to predict the reactions in the tundish. In the current study, a reaction model of the tundish was developed based on FactSage Macro Processing to predict the evolutions of steel chemistry and inclusion compositions in the tundish.

In the previous works,<sup>[15]</sup> it was proposed that the one-strand tundish can be divided into the mixing zone and the plug zone by the weir of the tundish. During the steady casting process, the molten steel firstly impinged the bottom of the tundish and flowed upward. The molten steel was strongly mixed in the mixing zone due to the large turbulence kinetic energy. Then, the molten steel flowed into the plug zone between the weir and the bottom. Whereafter, the molten steel uniformly flowed toward the outlet along the long wall in the plug zone. After that, the molten steel in the plug zone flowed toward the submerged entry nozzle from the outlet. The schematic diagram of the flow and the mixing process in a single-strand continuous casting tundish is shown in Figure 1. The mixing zone was set as the zone A. The melt volume in the plug zone was equally divided into zones B, C, and D. The calculation of time step can be reckoned by the melt volume in zone B divided by the teeming rate. In the schematic representation, the reactions R0–R5 occurred in each single time step represented the following:

R0: The air absorption of the incoming molten steel.  
R1: The incoming molten steel with the same volume of zone B was injected and mixed with the molten steel in zone A. The reacted molten steel was split into the equivalent molten steel in zone A, and the rest molten steel remained in the transient zone B'. R2: The molten steel in zone B' flowed and mixed with the remaining molten steel in zone B. The reacted molten steel was split into the equal volume molten steel in zone B and transient zone C'. R3: The molten steel in zone C' flowed

---

YING REN, LIFENG ZHANG, HAITAO LING, YI WANG, DONGTENG PAN, and QIANG REN are with the School of Metallurgical and Ecological Engineering, University of Science and Technology Beijing (USTB), Beijing 100083, P.R. China. XINCHENG WANG is with the School of Metallurgical and Ecological Engineering, University of Science and Technology Beijing (USTB), and also with the Xinjiang Bayi Iron and Steel Co., Ltd., Urumchi 830022, P.R. China. Contact email: zhanglifeng@ustb.edu.cn

Manuscript submitted December 9, 2016.

Article published online April 3, 2017.

and mixed with the remaining molten steel in zone C. The reacted molten steel was split into the equal volume molten steel in zone C and transient zone D'. R4: The molten steel in zone D' flowed and mixed with the remaining molten steel in zone D. The reacted molten steel was split into the equal volume molten steel in zone D and transient zone E'. R5: The rest molten steel in zone E' flowed toward the submerged entry nozzle from the outlet.

During the cast start and ladle change process, the incoming molten steel was oxidized by the air since the shroud was not submerged in the molten steel in the tundish, which was a primary factor responsible for the reoxidation of the molten steel in the tundish in the initial teeming stage and ladle change process.<sup>[6]</sup> The molten steel teemed from the ladle was shortly exposed in the air. It was assumed that the oxygen in the molten steel can be increased to a certain fixed level due to the absorption of oxygen from the air. When the level of the molten steel reached stability during the steady casting process, the shroud was submerged in the molten steel. Thus, it can be considered that there was no air reoxidation of the molten steel.

To simplify the model and calculation, the following assumptions are made in the current model: (1) The compositions of steel and inclusions in each reaction zone are homogenous; (2) Steel/inclusion reaction is assumed to reach the equilibrium; (3) The temperature can be maintained at a certain fixed temperature; (4) The removal of inclusions to the slag, slag/steel reaction, and the influence of refractory are not considered in the current model; (5) The effect of the dead zone on the steel/inclusion reaction is also ignored.

In the FactSage software, All the input conditions and output can be stored and passed to the different

equilibrium calculations or externally to a simple text file or Microsoft Excel™ worksheets using FactSage Macro Processing code. A small program can be written using this macro processing code for equilibrium calculations.<sup>[25]</sup> Thus, the calculation process of the current model is as follows: (1) The initial conditions (compositions and amounts of steel and inclusions, and the temperature) are set up using the Microsoft Excel™ as an interface. (2) Air absorption of the incoming molten steel in step R0; (3) The flow, mixing, and splitter of the molten steel and inclusions in steps R1 to R5; (4) The equilibrated conditions are output to the Microsoft Excel™. The above procedure is repeated until time *t* is a satisfied final time. The thermodynamic phase equilibria of all reactions were calculated using FactSage with FactPS, FToxid, and FTmisc databases.<sup>[22]</sup>

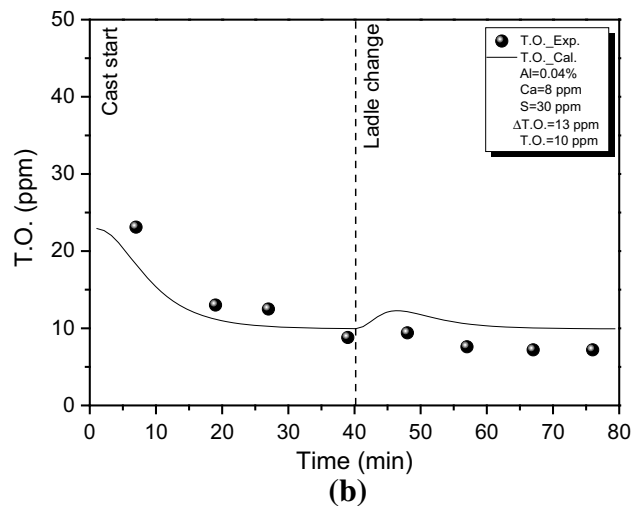
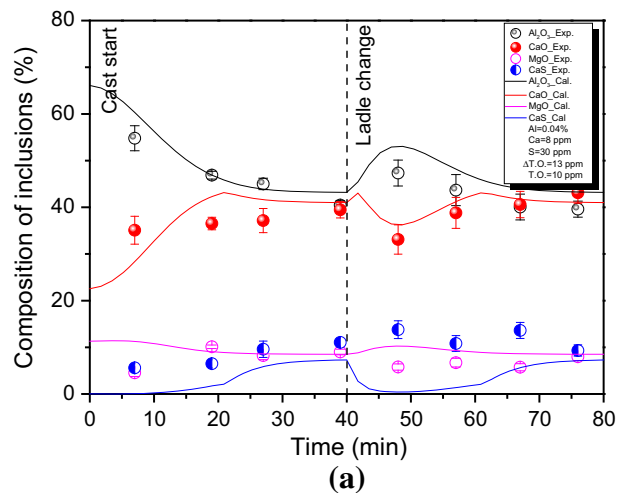


Fig. 2—Comparison of the predicted and experimental results of Ca-treated Al-killed steels in zone D of tundish. (a) Inclusion compositions, (b) T.O. in steel.

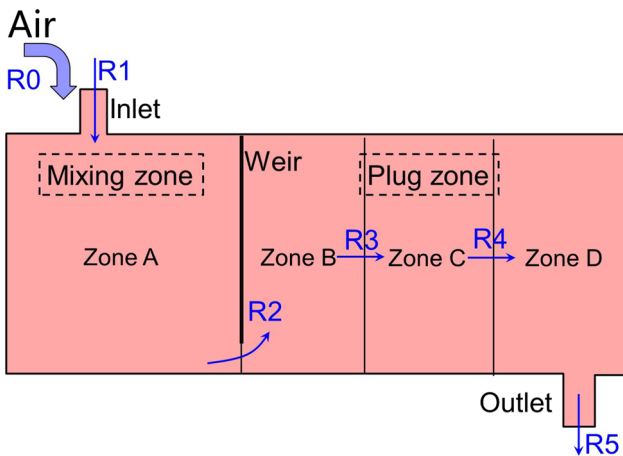


Fig. 1—Schematic diagram of reactions in continuous casting tundish.

Table I. Composition of the Steel Before Casting (Weight Percent)

C	Si	Mn	S	Al	T.O.	Ca	Mg	Fe
0.15	0.3	1.4	0.003	0.04	0.0010	0.0008	0.0005	balanced

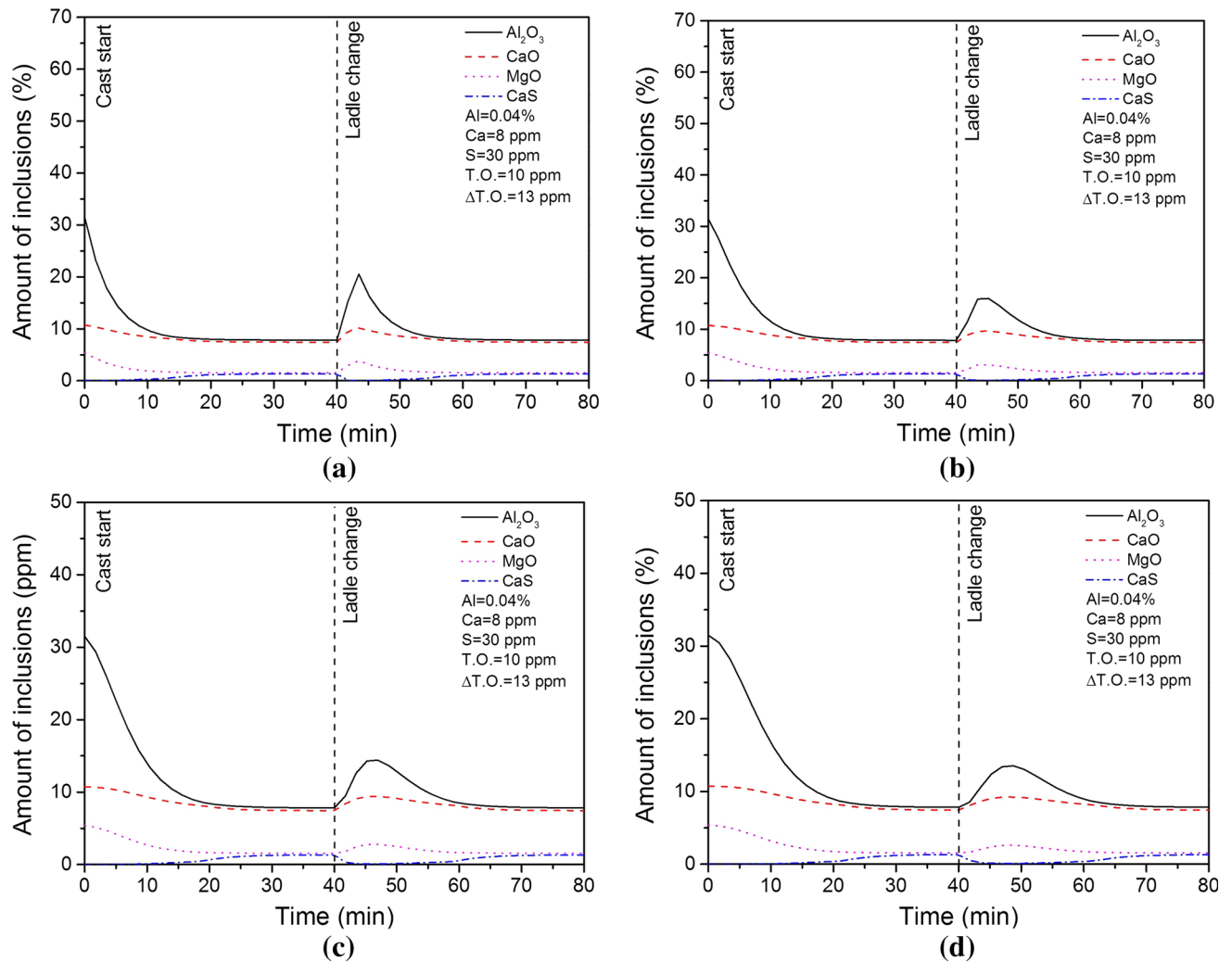


Fig. 3—The predicted inclusion compositions in various reaction zones of tundish: (a) Zone A, (b) Zone B, (c) Zone C, (d) Zone D.

To verify the accuracy of the developed model, the simulated results were validated with the industrial results. The Ca-treated Al-killed steel was teemed from an 115-ton ladle into a 25-ton tundish, and then poured into a single-strand continuous mold. The casting temperature was 1823 K (1550 °C). The initial state of the industrial tundish system was empty. The teeming time of each heat was 40 minutes. Then, the teeming rate was 2.875 tons per minute. It can be calculated that the duration of fully filling the tundish at cast start process was 8.7 minutes. The industrial data showed that the ladle change process lasted roughly 2 minutes. The volumes of the mixing zone and the plug zone were 40 and 60 pct of the total melt volume in the tundish. Thus, the time step was given as 104.35 seconds. To investigate the reoxidation behavior of the molten steel teemed from the ladle into the tundish, steel samples from a casting sequence with two heats were taken every 9–15 minutes. The samples were taken from a position in the tundish equivalent to Zone D. The inclusions in steel samples were analyzed using automated SEM/EDS inclusion analysis (ASPEX). At least 500 inclusions on each sample were detected using ASPEX to obtain the

composition of inclusions. In the current work, the working magnification of ASPEX was set at  $\times 400$  and the minimum detectable size of inclusions was 1.0  $\mu\text{m}$ . The total oxygen (T.O.) of the steel was analyzed using a Leco analyzer. The bulk chemical analysis of the steel was performed by a spark OES. The composition of the steel before casting is listed in Table I. The absorbed oxygen ( $\Delta\text{T.O.}$ ) in the teemed molten steel at cast start was measured to be 13 ppm.

The initial state of the modeled tundish system was empty. The composition of the incoming molten steel in FactSage is set as Table I. The air absorption was modeled in FactSage as a total oxygen increase. Therefore, the T.O. of the incoming steel during the 8.7 minutes cast start and the 2 minutes ladle change process is given as 23 ppm. Figure 2(a) shows the comparison of the measured inclusion compositions at the outlet and the predicted results of the zone D. Error bars represented the 95 pct confidence interval of the mean composition of inclusions. It should be noted that the current predicted inclusion compositions showed a good agreement with the measured results. It was demonstrated that the current reaction model can be used to

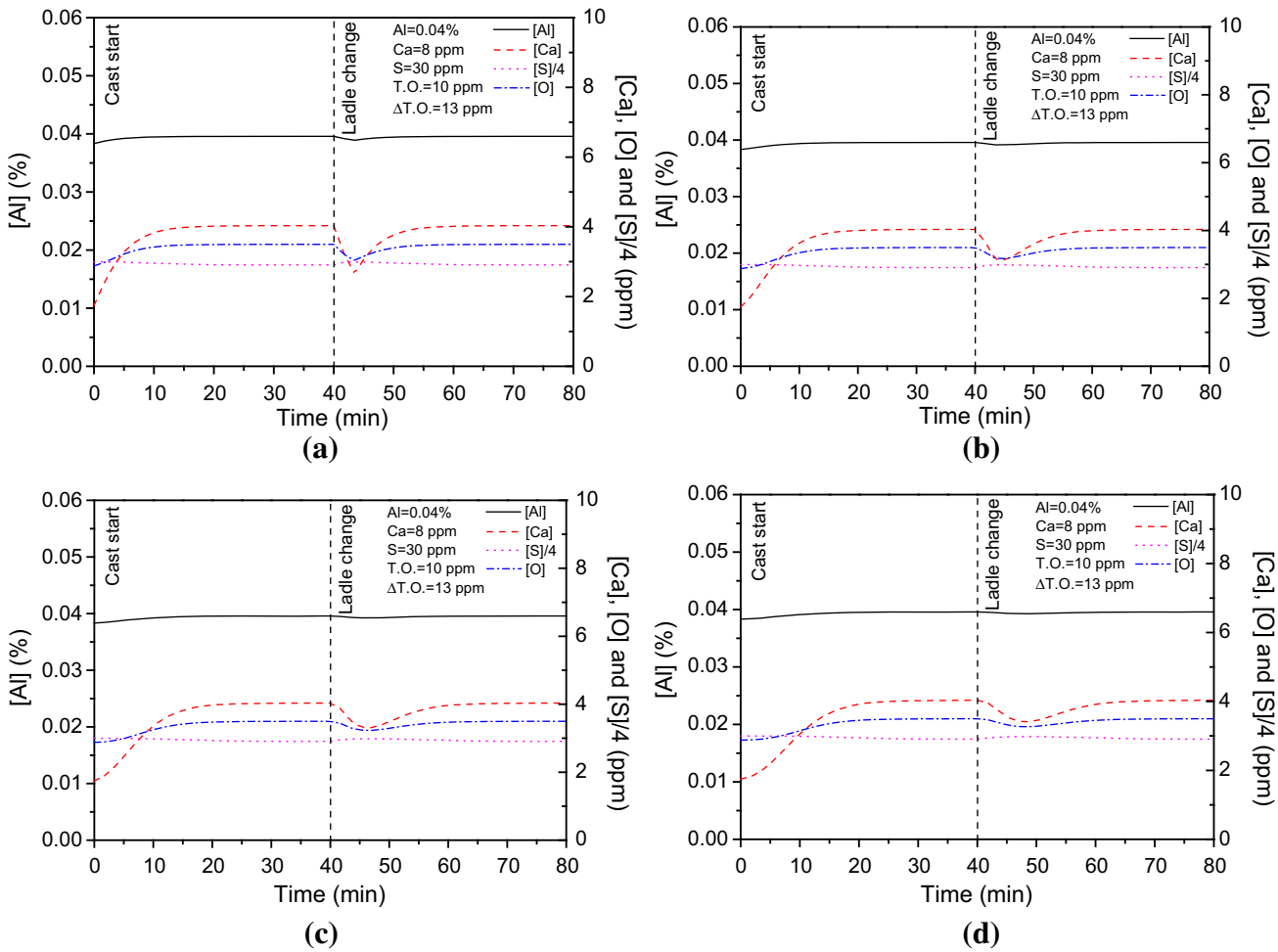


Fig. 4—The predicted steel compositions in various reaction zones of tundish: (a) Zone A, (b) Zone B, (c) Zone C, (d) Zone D.

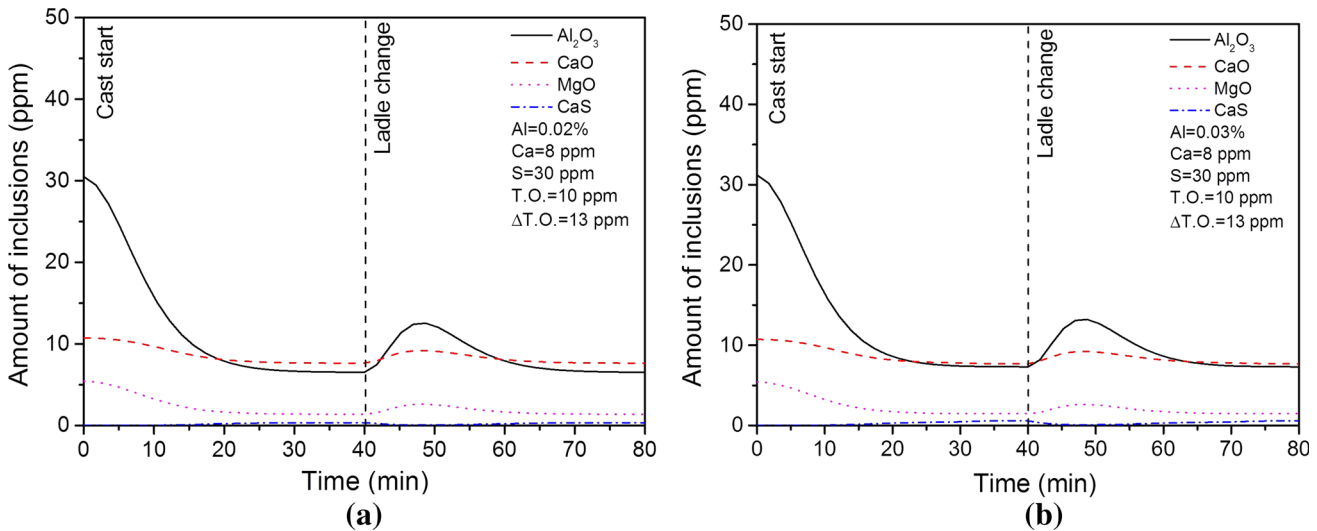


Fig. 5—Effect of Al on the evolution of inclusion compositions in zone D.

successfully predict the evolution of inclusion compositions in the tundish. It can be seen that the measured CaS in inclusions was higher than that of the predicted one, which may be caused by the precipitation of CaS

during the solidification and cooling process of the steel sample. Figure 2(b) shows the comparison of the measured T.O. at the outlet and the predicted results of the zone D. It can be seen that the predicted T.O.

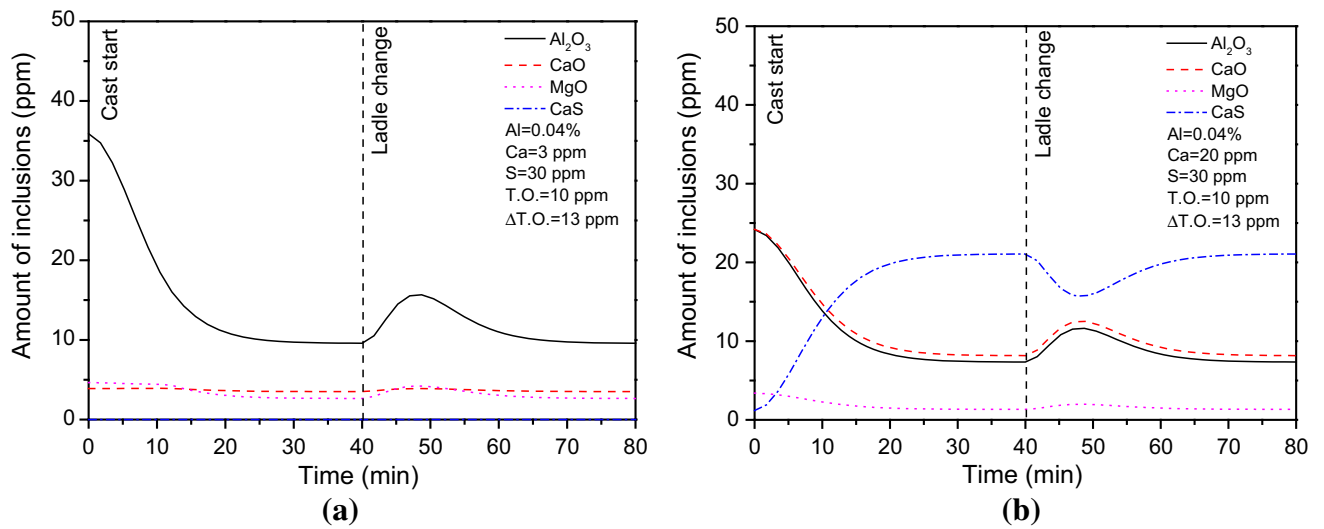


Fig. 6—Effect of Ca on the evolution of inclusion compositions in zone D.

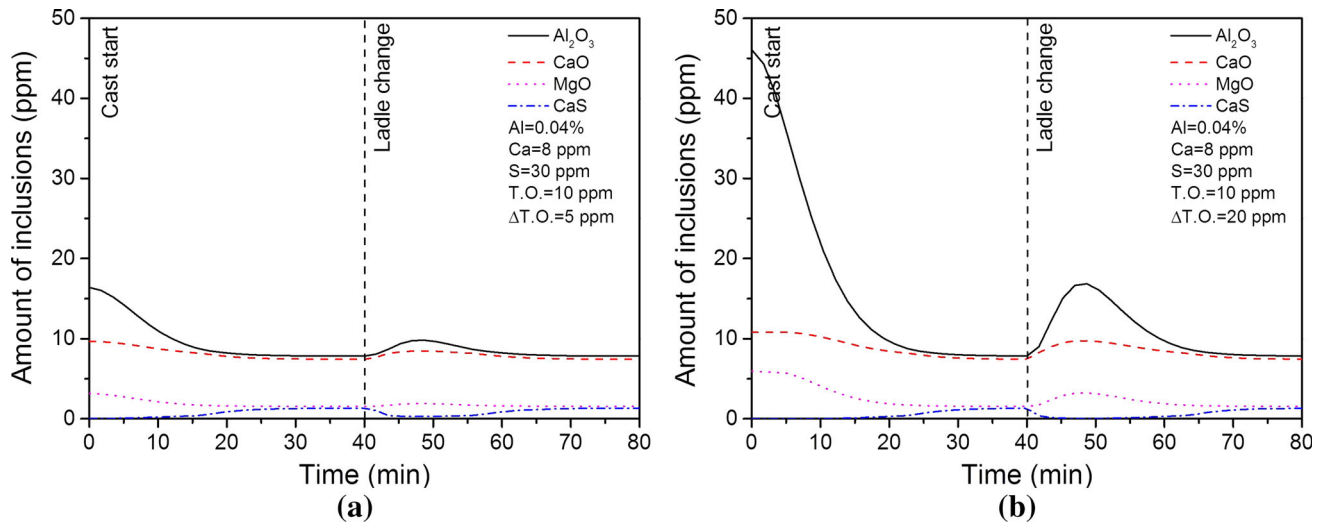


Fig. 7—Effect of  $\Delta T.O.$  on the evolution of inclusion compositions in zone D.

roughly showed a similar tendency with the experimental values. The difference of the experimental and predicted values may be caused by the neglect of the inclusion flotation in the tundish in the current model, which will be a focus of our future modeling studies.

Figure 3 shows the predicted inclusion compositions in various reaction zones of the tundish. During the steady casting process, the formed inclusions were  $Al_2O_3$ -CaO-rich oxides. At the cast start,  $Al_2O_3$  in inclusions increased from more than 8 ppm to more than 30 ppm caused by the reoxidation. Meanwhile, the CaO and MgO slightly rose up. Consequently, the CaO/ $Al_2O_3$  in inclusions distinctly declined during the reoxidation. The CaS in inclusions decreased to a low level due to the formation of CaO. During the ladle change process, the  $Al_2O_3$ , CaO, and MgO in inclusions significantly picked up. It can be seen that evolution of inclusion in various zones showed a similar tendency.

However, from the inlet to the outlet in tundish, it took a longer time for inclusions to reach stability during unsteady continuous casting. Figure 4 shows the predicted steel compositions in various reaction zones of the tundish. It can be seen that the [Al], [Ca], and [O] reduced due to the formation of oxides caused by the reoxidation during the cast start and ladle change process. Meanwhile, the [S] in steel slightly rose up since more Ca reacted with [O] and formed CaO.

To predict the evolution of inclusions in Ca-treated Al-killed steels with various steel compositions in the tundish, a large number of calculations were apace carried out using Factsage Macro Processing. Typically, the evolution of inclusion compositions in zone D was given in the following predicted results. Figure 5 shows the effect of Al on the evolution of inclusion compositions. Comparing Figures 5 and 3(d), with the Al in the steel increasing from 0.02 to 0.04 pct, the ratio of CaO/ $Al_2O_3$  in inclusions slightly went up. In Figure 6, the



modification of  $\text{Al}_2\text{O}_3$  and  $\text{MgO}$  in inclusions can be significantly promoted by increasing Ca from 3 to 30 ppm. The excess Ca led to the formation of CaS in inclusions. Meanwhile, the reoxidation during unsteady casting significantly increased the  $\text{Al}_2\text{O}_3$  in inclusions, while CaS in inclusions reduced due to the reoxidation of Ca in the steel. As shown in Figure 7, the reoxidation can promote the generation of  $\text{Al}_2\text{O}_3$ , CaO, and  $\text{MgO}$  in inclusions with the decreasing of CaS. The increase in  $\Delta T.O.$  during the cast start and ladle change obviously lowered the  $\text{CaO}/\text{Al}_2\text{O}_3$  in inclusions. Meanwhile, it took longer time for the oxidized inclusions to evolve to the normal ones.

In the current study, a reaction model was developed using Factsage Macro Processing, which can successfully predict the evolutions of steel chemistry and inclusion compositions during the reoxidation of Ca-treated Al-killed steels in the tundish. The reaction model was widely used to predict the evolution of inclusions during tundish reoxidation of Ca-treated Al-killed steels with varying concentrations of Al, Ca, and absorbed oxygen.

---

The authors are grateful for the support from the National Science Foundation China (Grant No. 51274034, No. 51334002, No. 51604023, No. 51504020, and No. 51404019), Beijing Key Laboratory of Green Recycling and Extraction of Metals (GREM), the Laboratory of Green Process Metallurgy and Modeling (GPM<sup>2</sup>) and the High Quality steel Consortium (HQSC) at the School of Metallurgical and Ecological Engineering at the University of Science and Technology Beijing (USTB), China.

## REFERENCES

1. J.H. Park and H. Todoroki: *ISIJ Int.*, 2010, vol. 50 (10), pp. 1333–46.
2. L. Zhang and B.G. Thomas: *ISIJ Int.*, 2003, vol. 43 (3), pp. 271–91.
3. Y. Ren, L. Zhang, W. Fang, S. Shao, J. Yang, and W. Mao: *Metall. Mater. Trans. B*, 2016, vol. 47B (2), pp. 1024–34.
4. S. Joo, J.W. Han, and R.I.L. Guthrie: *Metall. Mater. Trans. B*, 1993, vol. 24B (5), pp. 767–77.
5. L. Zhang, S. Taniguchi, and K. Cai: *Metall. Mater. Trans. B*, 2000, vol. 31B (2), pp. 253–66.
6. K. Sasai and Y. Mizukami: *ISIJ Int.*, 2000, vol. 40 (1), pp. 40–47.
7. K. Matsunaga, C. Namiki, and T. Araki: *Tetsu-to-Hagané*, 1973, vol. 59 (1), pp. 72–84.
8. Y. Habu, H. Kitaoka, Y. Yoshii, T. Emi, Y. Iida, and T. Ueda: *Tetsu-to-Hagané*, 1976, vol. 62 (14), pp. 1803–12.
9. S. Li, L. Zhang, Y. Ren, W. Fang, W. Yang, S. Shao, J. Yang, and W. Mao: *ISIJ Int.*, 2016, vol. 56 (4), pp. 584–93.
10. Y. Higuchi, Y. Tago, K. Takatani, and S. Fukagawa: *Tetsu-to-Hagané*, 1998, vol. 84 (5), pp. 333–38.
11. Y. Higuchi, Y. Tago, S. Fukagawa, T. Kanai, and A. Mutoh: *Tetsu-to-Hagané*, 1999, vol. 85 (5), pp. 375–81.
12. B. Coletti, B. Gommers, C. Vercruyssen, B. Blanpain, P. Wollants, and F. Haers: *Ironmak. Steelmak.*, 2003, vol. 30 (2), pp. 101–05.
13. N. Bessho, H. Yamasaki, T. Fujii, T. Nozaki, and S. Hiwasa: *ISIJ Int.*, 1992, vol. 32 (1), pp. 157–63.
14. H. Ling and L. Zhang: *JOM*, 2013, vol. 65 (9), pp. 1155–63.
15. D. Chen, X. Xie, M. Long, M. Zhang, L. Zhang, and Q. Liao: *Metall. Mater. Trans. B*, 2014, vol. 45B (2), pp. 392–98.
16. A.K. Sinha and Y. Sahai: *ISIJ Int.*, 1993, vol. 33 (5), pp. 556–66.
17. Y. Miki and B.G. Thomas: *Metall. Mater. Trans. B*, 1999, vol. 30B (4), pp. 639–54.
18. S. Yang, L. Zhang, J. Li, and K. Peaslee: *ISIJ Int.*, 2009, vol. 49 (10), pp. 1551–60.
19. L. Holappa, M. Hamalainen, M. Liukkonen, and M. Lind: *Ironmak. Steelmak.*, 2003, vol. 30 (2), pp. 111–15.
20. Y.-B. Kang and H.-G. Lee: *ISIJ Int.*, 2004, vol. 44 (6), pp. 1006–15.
21. Y.-B. Kang and A.D. Pelton: *Metall. Mater. Trans. B*, 2009, vol. 40B (6), pp. 979–94.
22. I.-H. Jung, S.A. Decterov, and A.D. Pelton: *ISIJ Int.*, 2004, vol. 44 (3), pp. 527–36.
23. A. Harada, N. Maruoka, H. Shibata, and S.-Y. Kitamura: *ISIJ Int.*, 2013, vol. 53 (12), pp. 2110–17.
24. P.R. Scheller and Q. Shu: *Steel Res. Int.*, 2014, vol. 85 (8), pp. 1310–16.
25. M.-A. Van Ende and I.-H. Jung: *Metall. Mater. Trans. B*, 2017, vol. 48 (1), pp. 28–36.
26. S.P.T. Piva, D. Kumar, and P.C. Pistorius: *Metall. Mater. Trans. B*, 2017, vol. 48 (1), pp. 37–45.
27. J.H. Shin, Y. Chung, and J.H. Park: *Metall. Mater. Trans. B*, 2017, vol. 48 (1), pp. 46–59.
28. J. Peter, K.D. Peaslee, D.G.C. Robertson and B.G. Thomas: *AISTech 2005*, AIST, Pittsburgh, PA, 2005, pp. 959–73.
29. Y. Ren, Y. Zhang, and L. Zhang: *Ironmak. Steelmak.*, 2016, pp. 1–8 (Published online).
30. M.-A. Van Ende, Y.-M. Kim, M.-K. Cho, J. Choi, and I.-H. Jung: *Metall. Mater. Trans. B*, 2011, vol. 42B (3), pp. 477–89.